Biochemical Pharmacology, Vol. 58, pp. 959–971, 1999.

ISSN 0006-2952/99/$–see front matter
PII S0006-2952(99)00190-2

Differential *In Vitro* Association of Vinca Alkaloid-Induced Tubulin Spiral Filaments into Aggregated Spirals

Pascal Verdier-Pinard, Michèle Garès and Michel Wright*
INSTITUT DE PHARMACOLOGIE ET DE BIOLOGIE STRUCTURALE, C.N.R.S., 31077 TOULOUSE CEDEX, FRANCE

ABSTRACT. Vinblastine, vincristine, vindesine, and vinorelbine, the four vinca alkaloids used in cancer therapy, differ in their antitumoral spectra and toxicities, but not in their inhibitory effects on microtubule assembly *in vitro*. At higher drug concentrations, vinca alkaloids induce the assembly of spiral filaments of tubulin, which, in turn, can interact laterally and form paracrystals. Using methods that distinguish spiral filaments and paracrystals (aggregated spirals), we found that spiral filament formation was largely independent of the incubation temperature, of the alkaloid used, and of the presence or absence of microtubule-associated proteins (MAPs). In contrast, the formation of aggregated spirals was markedly dependent on the alkaloid used, on the incubation temperature, and on the absence or presence of MAPs. Aggregated spirals failed to assemble in the presence of high concentrations of MAP-1A or MAP-1B, whereas they assembled readily with tau and MAP-2. Differences in patterns of turbidity development using pure tubulin allowed the classification of thirteen cytotoxic vinca alkaloids into five distinct groups, with centrifugal recovery of aggregated spirals in close agreement with the various turbidity patterns. With microtubule protein, i.e. tubulin preparations containing MAPs, only four groups were defined by turbidity patterns, and centrifugal protein recovery was more divergent. Vinblastine, vincristine, vindesine, and vinorelbine fell into distinct groups under both reaction conditions, and thus they appear to have qualitatively distinguishable *in vitro* interactions with tubulin. These differential effects on spiral filament and aggregated spiral assembly revealed that the four drugs induce different constraints on the tubulin molecule. BIOCHEM PHARMACOL **58**;6:959–971, 1999. © 1999 Elsevier Science Inc.

KEY WORDS. vinca alkaloids; tubulin; microtubule-associated proteins; paracrystals; spirals; turbidity

The microtubule cytoskeleton is considered the pharmacological target of the vinca alkaloids [1]. These complex molecules, formed by the association of a velbanamine moiety (modified catharanthine) and a vindoline moiety, bind specifically to tubulin [2, 3]. They induce the disassembly of cellular microtubules, most likely by modifying their dynamics [4, 5]. VLB†, VCR, VDS, and NVB are members of this class of drugs used in cancer therapy, and they differ in their antitumor and toxicity profiles [6] (see Table 1 for structures). Despite numerous investigations, these drugs appear to have similar actions at the tubulin level [7]. *In vitro*, they all prevent microtubule assembly in the micromolar range [7]. At higher concentrations these compounds induce the assembly of tubulin spiral filaments both *in vivo* and *in vitro* [2, 8] interacting laterally to form large ordered aggregates. Such aggregates are called paracrystals when their size and spiral order lead to birefringence properties under polarized light microscopy.

Studies have described variable effects of temperature and MAPs on turbidity development and aggregate morphology induced by vinca alkaloids. For instance, Mackinlay *et al.* [9] showed that, in the presence of 40 μM VLB, the turbidity of a solution of purified tubulin was markedly lower at 37° as compared with 0°. In agreement with this observation, Takanari *et al.* [10] showed that, at 4°, more paracrystals are formed in CHO cells in the presence of VLB than at 37°. Himes and colleagues [11] demonstrated morphological differences in VLB tubulin-induced aggregates with and without MAPs, and Ludueña and colleagues [12, 13] demonstrated differences in turbidity effects and aggregate morphology with tau versus MAP-2. These results imply that MAPs have important modulating effects on the aggregates induced by vinca alkaloids.

However, few comparative studies on the aggregates induced by different vinca alkaloids have been performed *in vitro* [7, 14, 15] and *in vivo* [16]. Our preliminary studies of the comparative effects of VCR, VLB, and two epimers of a VLB aminophosphonate derivative suggested that these compounds differ in their *in vitro* ability to induce aggregation of tubulin spiral filaments [17, 18]. These initial findings prompted us to examine additional vinca alkaloids

* Corresponding author: Dr. Pascal Verdier-Pinard, NIH, NCI, Laboratory of Drug Discovery Research and Development, Bldg. 37, 5D02, 9000 Rockville Pike, Bethesda, MD 20892. Tel. (301) 496-4855; FAX (301) 496-5839; E-mail: verdierp@dc37a.nci.nih.gov

† *Abbreviations*: VLB, vinblastine; VCR, vincristine; VDS, vindesine; NVB, vinorelbine; PIPES, 1,4-piperazinediethanesulfonic acid; DTT, dithiothreitol; PMSF, phenylmethylsulfonyl fluoride; SAV, *S*-anhydrovinblastine; RAV, *R*-anhydrovinblastine; MAPs, microtubule-associated proteins; and aminoacid code(P)-$(R)_2$, aminophosphonate diester.

Received 10 September 1998; accepted 26 January 1999.

TABLE 1. Chemical structures

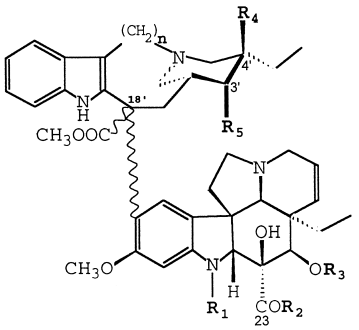

Compounds	Abv	n	R_1	R_2	R_3	R_4	R_5	$C_{18'}$
Vinblastine	VLB	2	CH_3	OCH_3	$COCH_3$	OH	H	S
Vincristine	VCR	2	CHO	OCH_3	$COCH_3$	OH	H	S
Vindesine	VDS	2	CH_3	NH_2	H	OH	H	S
Vinorelbine	NVB	1	CH_3	OCH_3	$COCH_3$	Δ3′-4′*		S
18′-*S*-Anhydrovinblastine	SAV	2	CH_3	OCH_3	$COCH_3$	Δ3′-4′*		S
18′-*R*-Anhydrovinblastine	RAV	2	CH_3	OCH_3	$COCH_3$	Δ3′-4′*		R
S-12363	**63**	2	CH_3	*l*-Val(P)-$(OC_2H_5)_2$	H	OH	H	S
S-12362	**62**	2	CH_3	*d*-Val(P)-$(OC_2H_5)_2$	H	OH	H	S
S-12335	**35**	2	CH_3	*l*-Ala(P)-$(OC_2H_5)_2$	H	OH	H	S
S-12334	**34**	2	CH_3	*d*-Ala(P)-$(OC_2H_5)_2$	H	OH	H	S
S-12129	**29**	2	CH_3	*l*-Tryp(P)-$(OC_2H_5)_2$	H	OH	H	S
S-12128	**28**	2	CH_3	*d*-Tryp(P)-$(OC_2H_5)_2$	H	OH	H	S
S-12155	**55**	2	CH_3	*dl*-α-*n*-pentyl-Gly(P)-$(OC_2H_5)_2$	H	OH	H	S
S-12156	**56**	2	CH_3	*dl*-Asp(P)-$(OC_2H_5)_3$	H	OH	H	S

*Double bond.

and the effects of various reaction components on formation of aggregated spirals.

In the present study, we observed differences in the effects of NVB, VLB, VCR, VDS, and aminophosphonate VDS derivatives in inducing the aggregation of spirals, as a function of incubation temperature, and in the presence or absence of MAPs. Additionally, we isolated the main neuronal MAPs, i.e. tau, MAP-2, MAP-1A, and MAP-1B, and we examined whether they were promoting or inhibiting the aggregation of spirals.

MATERIALS AND METHODS

Vinca *Alkaloids*

VLB and VCR sulfates were obtained from Dehors Laboratories, VDS sulfate from Lilly, NVB from Pierre Fabre Laboratories, and the VDS α-aminophosphonate derivatives from Servier Laboratories [19]. 18′*S* and 18′*R* anhydrovinblastine were obtained from the Institut de Chimie des Substances Naturelles (ICSN-CNRS). All vinca alkaloids were dissolved in water:ethanol (1:1). The maximal concentration of ethanol in the assays was less than 0.5%, which does not induce tubulin aggregation.

Microtubule Protein

A sheep brain microtubule protein preparation was obtained by two cycles of assembly/disassembly of microtubules [20] and was stored at −80° until used. This preparation was used for the purification of tubulin, or it was resuspended in buffer 1 (100 mM PIPES, 1 mM EGTA, 0.5 mM $MgCl_2$, pH 6.9) containing 1 mM GTP and stored in liquid nitrogen. Prior to use, aliquots were thawed and centrifuged for 5 min at 21,000 *g*. SDS–PAGE showed that these microtubule protein preparations contained about 85% tubulin.

Preparation of Pure Tubulin and MAPs

Tubulin and MAPs were separated by phosphocellulose chromatography [21] (40 mg of microtubule protein, 13 × 0.9 cm column, flow rate 0.7 mL/min). Pure tubulin was recovered in the void volume (6–10 mg/mL); MAPs were eluted with 0.5 M NaCl, dialyzed, and concentrated (4–5 mg/mL) on Centriprep 30 (Amicon, 1200 *g*). Fractions were adjusted to 1 mM GTP and 0.5 mM $MgCl_2$ and were stored in liquid nitrogen. Alternatively, MAP-1 was separated from MAP-2 and tau by modifications of the method of Fujii *et al.* [22]. Microtubule proteins (14 mg/mL), in buffer 1 containing 1 mM DTT, 0.5 mM PMSF, 10 μg/mL of pepstatin, 10 μM paclitaxel, and 22 μg/mL of poly-l-aspartic acid (31 kDa, from the Sigma Chemical Co.) were incubated for 30 min at 37° and centrifuged for 30 min at 120,000 *g* at 20°. The pellet was resuspended and recentrifuged, and the two supernatants containing MAP-1 were pooled. The pellet, resuspended in buffer 1 containing 1 mM DTT, 0.5 mM PMSF, 10 μg/mL of pepstatin, 10 μM

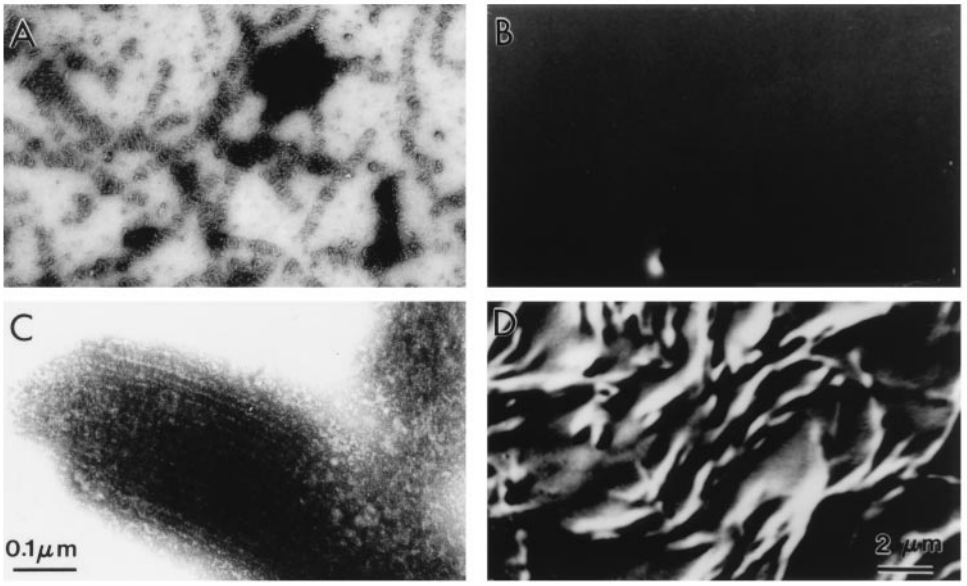

FIG. 1. Electron microscopic (A, C) and interference contrast microscopic (B, D) observations of abnormal polymers assembled in the presence of NVB (A, B) and compound 63 (C, D). Microtubule protein (2.8 mg/mL) was incubated for 1 hr in the presence of 100 μM NVB or 63 at 37°. In B, focusing was done on an air bubble.

paclitaxel, and 0.35 M NaCl was incubated for 30 min at 37° and centrifuged. The supernatant, containing tau and MAP-2, was concentrated and desalted on Centriprep 30. To eliminate residual tubulin, the two previous fractions were further chromatographed on a phosphocellulose column (1.6 x 8 cm, flow rate 0.5 mL/min, with the MAPs eluted with buffer 1 containing 0.5 M NaCl, 1 mM DTT, 0.5 mM PMSF, and 10 μg/mL of pepstatin). MAPs fractions were concentrated and desalted on Centricon 30, filtered through a Millex filter from Millipore, and chromatographed separately (3–4 mg of protein) on a Waters Pak 8HR Q minicolumn (flow rate 1 mL/min, FPLC Waters 650 E), with elution by a NaCl linear gradient in buffer 1 (tau was recovered in the void volume, while MAP-2 was eluted by 0.4 to 0.5 M NaCl; MAP-1A and MAP-1B were eluted with 0.65 to 0.75 M NaCl and 0.80 to 0.90 M NaCl, respectively). After concentration and dialysis on Centriprep 30, fractions were stored in liquid nitrogen until used (0.5 mg of MAP-1A or MAP-1B, 0.2 to 0.4 mg of tau or MAP-2). The purity and identity of the different fractions were checked by SDS–PAGE as described by Bloom *et al.* [23].

Microscopy

Aggregated spirals were observed directly by interference contrast microscopy [18]. In their absence, impurities and air bubbles were used to focus the objective. Electron microscopy was performed as described previously [18].

Sedimentation Assays

An air-driven ultracentrifuge (Beckman "Airfuge," rotor type 30°) was used in all sedimentation assays either in the cold room, following incubations at 0°, or at room temperature, following incubations at 37°. Pellets were resuspended in 0.1 mL of 3% Na_2CO_3, 0.1 M NaOH, and protein recovery was determined by the Lowry procedure.

Turbidimetric Assays

Change in absorbance due to light scattering following aggregate formation from microtubule protein or pure tubulin was determined at 0° and 37° in buffer 1 as described previously [18]. The temperature shifts from 0° to 37° and from 37° to 0° were completed in 3 min.

RESULTS

Differential Formation of Spiral Filaments and of Larger Aggregates Formed by the Association of Spiral Filaments

The addition of high concentrations of active vinca alkaloids to pure tubulin and to microtubule protein preparations (tubulin and MAPs) generally leads to an increase in turbidity, concomitantly with the appearance of spiral filaments and larger aggregates probably formed by the association of these filaments. The increase in turbidity could result from the formation of filaments, from their association into larger aggregates, or from a combined effect. An important exception to this generalization, however, is NVB, which, as will be shown below, causes little change in the turbidity of solutions of either microtubule protein or tubulin.

Initial electron microscopic studies at 37° with microtubule protein and the active derivatives shown in Table 1 demonstrated an array of complex aggregates, similar to those described by other workers, but, with NVB, complex aggregates were not prominent. Instead, most of the aberrant polymerization products consisted of single spiral filaments (Fig. 1A). We turned to interference contrast microscopy for additional information. No structures were

ever visualized with NVB (Fig. 1B), but with every other compound at 0°, and with most compounds at 37°, aggregates were clearly visible. The aggregates were most uniform with compound **63** (Fig. 1D), and the corresponding electron microscopic appearance of the aggregate is shown in Fig. 1C.

Therefore, we attempted to develop a centrifugal method to distinguish spiral filaments from aggregated spirals, using reaction mixtures containing microtubule protein and treated for 1 hr at 37° with NVB or **63** as model compounds inducing relatively homogeneous populations of filaments or aggregates, respectively. After only 3 min of centrifugation at 21,000 *g*, the pellets from reaction mixtures containing **63** were large, and the supernatants were free of protein. In contrast, with NVB, the same result was obtained only with centrifugation for 30 min at 126,000–178,000 *g*.

Most likely, this difference results from the state of aggregation induced by NVB and compound **63**. This hypothesis suggests, first, a quantitative relationship between turbidity and the amount of aggregated spirals, and, second, the absence of a correlation between turbidity and the amount of spiral filaments.

Indeed, when microtubule protein (2.8 mg/mL) was incubated in the presence of a 100 μM concentration of **63**, a turbidity of 0.8 A_{400} unit was observed. After centrifugation for 5 min at 21,000 *g* (sedimentation of aggregated spirals), the turbidity of the supernatant dropped to 0.09 A_{400} unit, a value close to that (0.05 A_{400} unit) observed in the presence of 100 μM NVB without previous centrifugation. Supporting our second assumption was the finding that prolonged centrifugation of the NVB samples (178,000 *g* for 30–60 min) yielded pellets as large as those obtained in brief centrifugations with **63** (2.2 and 2.3 mg/mL of sedimentable protein, respectively).

In summary, these initial experiments with **63** and NVB indicated that a combination of turbidimetric analysis with differential ultracentrifugation could be used to distinguish spiral filaments and possibly very small aggregates from larger aggregates induced by incubating tubulin preparations with active vinca alkaloids. Therefore, we decided to examine the potential of these methods with an active series of phosphonate vinca derivatives (structures in Table 1) with comparison to NVB and the other three vinca agents used in human patients: VLB, VCR, and VDS. Based on the preliminary results obtained with NVB and **63**, we defined aggregated spirals as material sedimenting after 5 min at 21,000 *g* and giving rise to a turbidity increase, and spirals as material sedimenting after 30 min at 178,000 *g* and yielding minimal turbidity signal.

Differentiation of Five Groups of Vinca *Alkaloids by Their Turbidity Patterns and Low Speed Centrifugal Recovery of Protein in the Presence of Pure Tubulin*

We initiated our detailed study with vinca derivatives by examining their effects on the aggregation of pure tubulin. Experiments involved two successive incubations at different temperatures: either at 0° followed by 37° (Fig. 2, left panels), or, alternatively, at 37° followed by 0° (Fig. 2, right panels). In these experiments, pure tubulin was incubated with a 5.5-fold equivalent of vinca alkaloid to assure maximum aggregate formation. In addition, formation of large tubulin aggregates, assumed to represent aggregated spirals, was quantitated by centrifugation for 5 min at 21,000 *g* at each temperature (Table 2). The specificity of the action of vinca alkaloids was checked by including in the study the active SAV and its inactive epimer RAV (structures in Table 1), which has no inhibitory effect on microtubule assembly [24]. A relatively nonspecific protein precipitation by VLB [25] or SAV is unlikely, since inactive RAV at 100 μM failed to yield protein that could be recovered by centrifugation (Table 2) or to cause a change in turbidity at 0° and 37° (Fig. 2A). This is in agreement with the observations of Ventilla *et al.* [26].

VLB and SAV, but none of the phosphonate derivatives, caused significant turbidity development at 0° but not 37°, in whatever order the incubation was performed (Fig. 2B). That the variations in turbidity during temperature shifts represented changes in extent of spiral aggregation was confirmed by the centrifugation assay, which resulted in substantially greater protein recovery at 0° (Table 2). In agreement with the preliminary observations presented above, the total amounts of tubulin spirals (individual filaments and assembled into aggregates) in the presence of VLB at 0° and at 37° were not significantly different (1.4 and 1.3 mg/mL, respectively, at 178,000 *g* for 30 min).

Besides the turbidity patterns obtained with VLB and SAV, the studies presented in Fig. 2 yielded four additional patterns (panels C–F). In the presence of the VDS class, a temperature shift did not affect turbidity greatly, nor, for the most part, did it affect the amount of aggregated spirals recovered by centrifugation significantly. Except with compound **56**, the final turbidity readings were independent of temperature order. With **56,** turbidity was about 3-fold higher if 0° was the initial incubation temperature, as opposed to an initial 37° incubation. Turbidity development was much more rapid at 0° than at 37° with VDS, compound **55**, and compound **56**.

The third turbidity pattern was obtained with NVB and a single phosphonate derivative, compound **62** (Fig. 2D), where no increase in turbidity occurred at either 0° or 37° regardless of order. Moreover, with both agents, no protein was recovered by centrifugation at 21,000 *g* for 5 min (Table 2). However, unlike RAV, both NVB [24] and **62** [18] inhibit microtubule assembly at low concentrations. Moreover, no aggregated spirals were observed with NVB and **62** at either temperature by interference and electron microscopy. Nevertheless, centrifugation at 178,000 *g* for 30 min yielded large amounts of spiral filaments (1.8 and 1.7 mg/mL with NVB at 0° and 37°, respectively, and 1.2 mg/mL with **62** at both 0° and 37°).

The fourth turbidity pattern was observed with VCR and two phosphonate derivatives, compounds **29** and **34** (Fig.

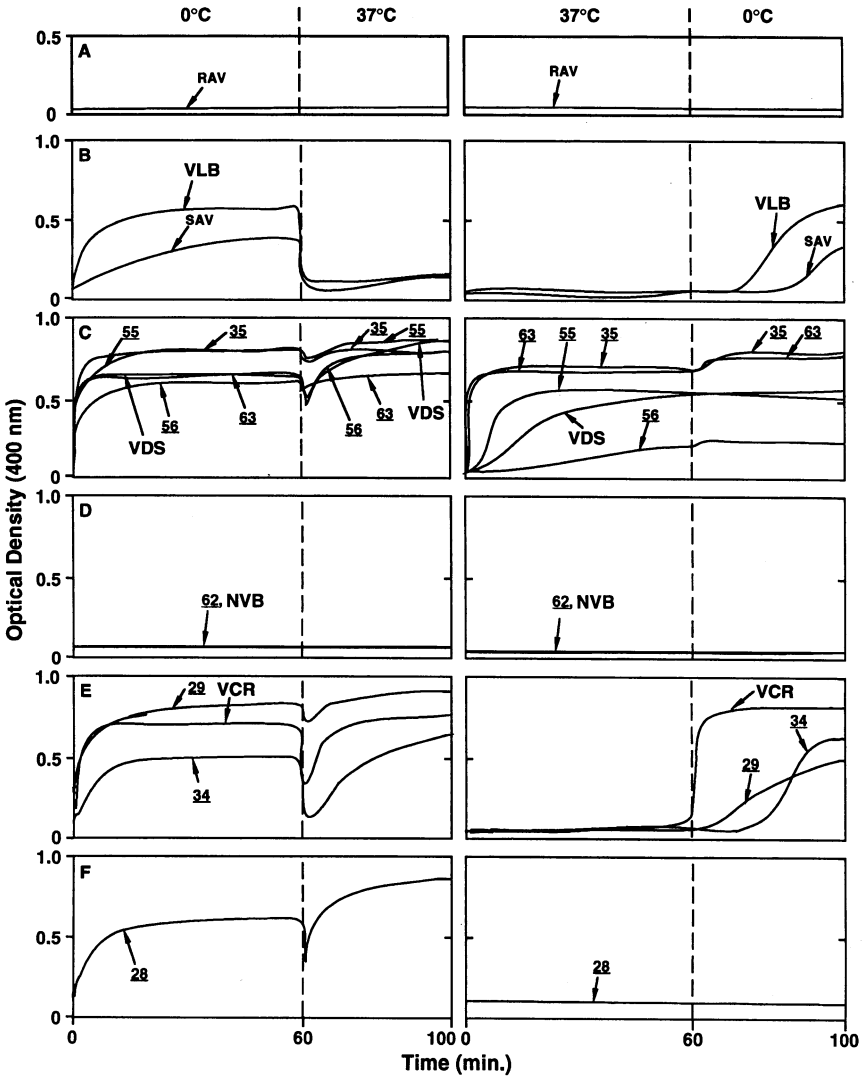

FIG. 2. Turbidity patterns obtained with pure tubulin with different vinca alkaloids. Tubulin (1.8 mg/mL; 18 μM) and vinca alkaloids (100 μM) were mixed at 0° or at 37° and immediately placed in the thermostatically controlled cuvette at the initial incubation temperature. The same tubulin preparation was used in all experiments presented in the figure. Left column: initial incubation at 0° and subsequent incubation at 37°. Right column: initial incubation at 37° and subsequent incubation at 0°. (A) RAV. With this inactive derivative there was no microtubule assembly in the absence of MAPs, since the critical concentration of tubulin under this reaction condition is greater than 1.8 mg/mL (data not presented). Results with the active alkaloids are presented in groups to emphasize the different turbidity patterns obtained (panels B–F). Typical results of at least three experiments are presented.

2E). In this group, when the initial incubation was at 0°, the transition to 37° resulted either in no significant change in turbidity or in a transient drop with initial recovery to the 0° level (similar to what was observed in the VDS group). However, when the initial incubation temperature was 37°, no turbidity development occurred until the temperature was reduced to 0° (similar to what was observed in the VLB group). When 0° followed 37°, turbidity development was much more rapid with VCR than with the two phosphonate derivatives. For the most part, centrifugal protein recovery was consistent with the turbidity results (Table 2). With VCR, however, a disproportionately large pellet was obtained following the initial 37° incubation. This may have resulted from an unintended cooling of the reaction mixture, since centrifugation was at room temperature. This could be a limitation of our method for vinca alkaloids such as VCR, which induced a fast aggregation of spirals when the temperature was shifted from 37° to 0°.

The fifth and last turbidity pattern was observed only with the phosphonate derivative **28** (Fig. 2F). With an initial 0° incubation, turbidity persisted at 37° (similar to the VDS group); but with the initial 37° incubation, no turbidity development occurred subsequently at 0° (similar to the NVB group). Centrifugal recovery of protein was consistent with the turbidity patterns (Table 2).

Differentiation of Four Groups of Vinca *Alkaloids by Their Turbidity Patterns in the Presence of Microtubule Protein*

From the above studies, with pure tubulin the formation of large complexes of aggregated spirals depended both on the specific vinca alkaloid examined and on the specific incubation temperature(s) used. To examine the influence of MAPs, we examined the action of the different derivatives with brain microtubule protein, as described above with pure tubulin. Roughly the same ratio of vinca alkaloid: tubulin used in the presence of pure tubulin was used.

As with pure tubulin, the inactive RAV did not induce formation of tubulin aggregates at 0°, and, as expected, it did not inhibit microtubule assembly at 37° (Fig. 3A; Table

TABLE 2. Effects of temperature shifts on the centrifugal recovery of aggregated spirals with pure tubulin

	Incubation at 0°, then at 37° Sedimentable protein*†		Incubation at 37°, then at 0° Sedimentable protein*‡	
Compound	**0°**	**37°**	**37°**	**0°**
RAV§	0.0	0.0	0.0	0.0
VLB	0.9	0.3	0.0	0.6
SAV	0.6	0.1	0.0	0.6
VDS	1.3	1.3	1.2	1.3
35	1.3	1.2	1.3	1.3
55	1.1	1.1	1.7	1.0
56	1.2	1.2	0.6	1.0
63	1.4	1.2	1.1	1.3
NVB	0.0	0.0	0.0	0.0
62	0.0	0.0	0.0	0.0
VCR	1.3	1.1	1.0	1.4
29	1.1	1.1	0.2	1.0
34	0.9	1.0	0.1	0.8
28	1.0	1.1	0.2	0.2

*Protein sedimented (mg/mL) at 21,000 *g* for 5 min at the end of each incubation period presented in Fig. 2.

†Correlation coefficients between the amounts of aggregated spirals and turbidity for all compounds studied were 0.95 at 0° and 0.97 at 37°.

‡Correlation coefficients between the amount of aggregated spirals and turbidity for all compounds studied were 0.79 at 37° and 0.76 at 0°.

§Inactive vinca alkaloid unable to prevent microtubule assembly.

3). Formation of microtubules was confirmed by electron microscopy (data not presented).

VLB and SAV, the active epimer of RAV, yielded turbidity patterns with microtubule protein (Fig. 3B) similar to those obtained with pure tubulin (Fig. 2B), except that with both compounds the 0° reaction following the incubation at 37° for 1 hr was more rapid with microtubule protein. The centrifugal results, however, were more divergent. With microtubule protein, pellets obtained at 37° were disproportionately large relative to the low turbidity readings, although they were smaller than the 0° pellets (Table 3). We cannot exclude the possibility that the 37° pellets are unexpectedly large due to cooling during centrifugation at room temperature as mentioned above with VCR in the presence of pure tubulin (note that in the presence of microtubule protein no lag time was observed after shifting the temperature to 0°, Figs. 2B and 3B). The SAV and VLB pellets were of similar size.

Similarly, VDS and the phosphonate derivatives **35**, **55**, **56**, and **63** yielded turbidity patterns (Fig. 3C) quite similar to those obtained with pure tubulin (Fig. 2C). The major difference occurred with compound **56** in the 37° to 0° transition. With microtubule protein, the turbidity reading was much higher than with pure tubulin and was comparable to that observed with the other compounds. Overall, the microtubule protein pellets obtained with these compounds were comparable in size at both temperatures (Table 3), independent of temperature order, as had been the case generally with pure tubulin. Note, however, that the largest pellets generally were obtained with compound **63**.

With NVB and microtubule protein (Fig. 3D) there was a slight increase in turbidity at 0° but not at 37°, different from the complete absence of turbidity change observed with pure tubulin and NVB (Fig. 2D). Nevertheless, NVB produced the least turbidity with microtubule protein of all the active compounds examined. The pellets obtained with NVB and microtubule protein were also relatively small (Table 3) compared to those obtained with the other vinca derivatives. The 0° pellets were significantly larger than the 37° pellets, but at both temperatures the NVB pellets with microtubule protein (Table 3) were much larger than the NVB pellets with pure tubulin (Table 2).

The turbidity patterns with VCR and microtubule protein (Fig. 3E) were almost indistinguishable from those with VCR and pure tubulin (Fig. 2E). The protein pellets with VCR and microtubule protein (Table 3) were also similar to those obtained with VCR and pure tubulin (Table 2), including the disproportionately large pellet (relative to the low turbidity reading) recovered after the initial 37° incubation.

Four of the phosphonate derivatives, however, displayed major changes in the turbidity patterns they induced when the reactions with microtubule protein were compared to those with pure tubulin. With pure tubulin, the effects of compound **62** had been indistinguishable from those of NVB (Fig. 2D). With microtubule protein, the patterns obtained with **62** were similar to those obtained with VLB (Fig. 3B). Curiously, the pellets obtained with microtubule protein and **62** at 37° were comparable in size to those obtained with NVB rather than VLB (Table 3). Moreover, by interference contrast microscopy, structures were ob-

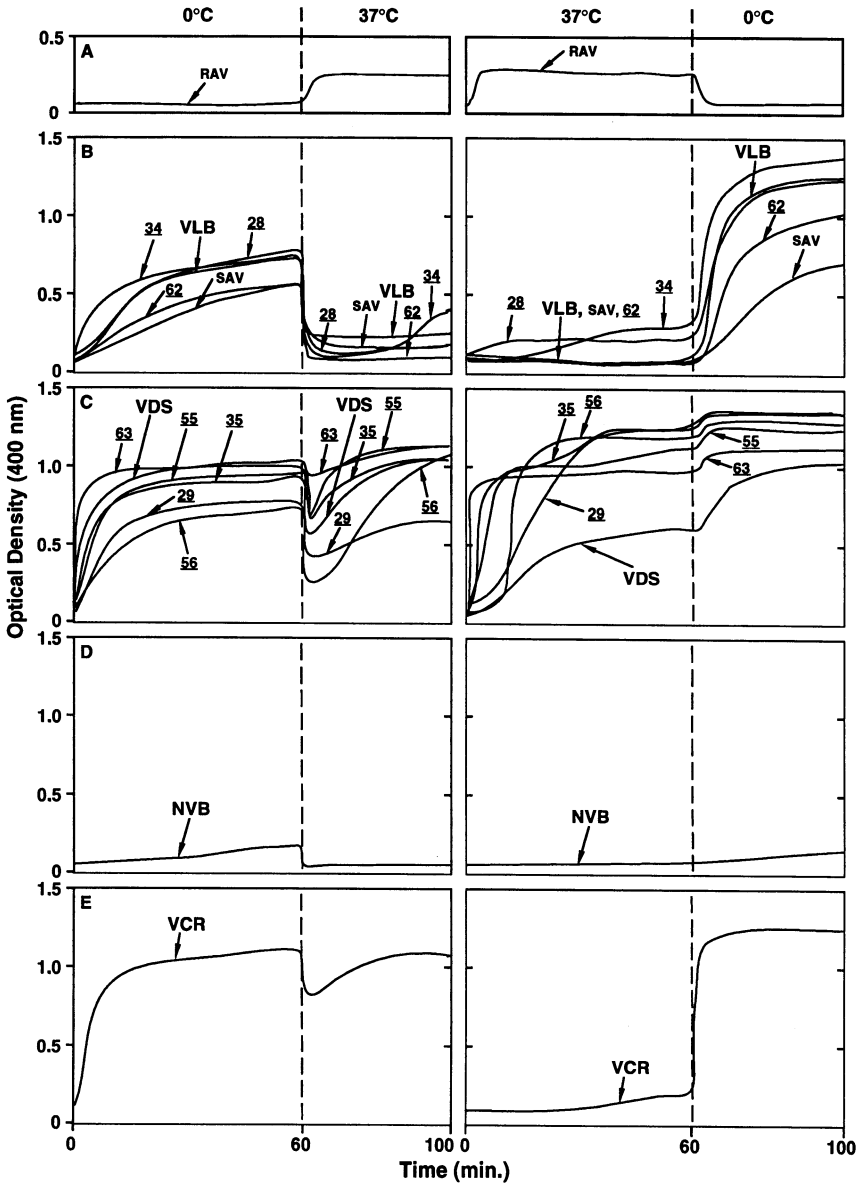

FIG. 3. Turbidity patterns obtained with microtubule protein with different vinca alkaloids. Microtubule protein (2.8 mg/mL) and vinca alkaloids (100 μM) were mixed at 0° or at 37° and placed immediately in the thermostatically controlled cuvette at the initial incubation temperature. The same microtubule protein preparation was used in all experiments presented in the figure. Left column: initial incubation at 0° and subsequent incubation at 37°. Right column: initial incubation at 37° and subsequent incubation at 0°. (A) RAV. With this inactive derivative, standard assembly reactions were observed: microtubule assembly at 37°, microtubule disassembly at 0°. Results with the active alkaloids are presented in groups to emphasize the different turbidity patterns obtained (panels B–E). Typical results of at least three experiments are presented.

served at 37° with VLB but not with NVB or **62** (data not presented). Compound **28**, which with pure tubulin had a unique turbidity pattern (Fig. 2F), had a turbidity pattern most like that observed with VLB with microtubule protein (Fig. 3B). Similarly, compound **34**, which with pure tubulin produced a VCR turbidity pattern (Fig. 2E), had a turbidity pattern resembling that obtained with VLB and microtubule protein (Fig. 3B). With microtubule protein these compounds induced much higher readings at 0° than at 37°. With **28** and **34,** the pellets recovered in the microtubule protein studies were also similar to those obtained with VLB, the 0° pellets being somewhat larger than the 37° pellets (Table 3). Finally, compound **29**, which with pure tubulin had produced a VCR turbidity pattern (Fig. 2E), had a turbidity pattern like that observed in the VDS group with microtubule protein (Fig. 3C). There was little change, as a function of temperature, in the final turbidity reading, or in protein recovered by centrifugation (Table 3).

Effects of Total MAPs on the Formation of Aggregated Spirals

Overall, the above studies show that our initial correlation, obtained with microtubule protein and compound **63** at 37°, of turbidity development with formation of readily sedimented aggregated spirals, held up better with pure tubulin than with microtubule protein. Nevertheless, in terms of turbidity patterns as a function of temperature, we found that each of the four vinca alkaloids used to treat human cancers yielded similar turbidity patterns with the two protein preparations. Moreover, virtually all phosphonate analogs that we examined induced turbidity patterns that fit into one of the groups represented by VLB, VCR, VDS, and NVB, although in a few cases the exact group changed when microtubule protein was used instead of pure tubulin, indicating a possible influence of MAPs.

We examined the four prototypical compounds (VLB,

TABLE 3. Effects of temperature shifts on the centrifugal recovery of aggregated spirals with microtubule protein

	Incubation at 0°, then at 37° Sedimentable protein*‡		Incubation at 37°, then at 0° Sedimentable protein*‡§	
Compound	**0°**	**37°**	**37°**	**0°**
RAV‖	0.1	1.1¶	1.5¶	0.0
VLB	1.1 (+)	0.8 (+)	0.8 (−)	1.7 (+)
SAV	1.1 (+)	0.8 (+)	0.7 (−)	1.3 (+)
28	0.9 (+)	0.6 (+)	0.7 (−)	1.3 (+)
34	1.0 (+)	0.8 (+)	0.9 (+)	1.5 (+)
62	1.0 (+)	0.3 (−)	0.3 (−)	1.3 (+)
VDS	1.3 (+)	1.5 (+)	2.0 (+)	1.6 (+)
29	1.0 (+)	1.4 (+)	1.5 (+)	1.6 (+)
35	1.2 (+)	1.8 (+)	2.0 (+)	1.5 (+)
55	1.4 (+)	1.8 (+)	1.6 (+)	1.5 (+)
56	1.1 (+)	1.5 (+)	1.8 (+)	1.6 (+)
63	1.3 (+)	2.0 (+)	2.2 (+)	2.1 (+)
NVB	0.7 (−)	0.2 (−)	0.3 (−)	0.5 (−)
VCR	1.3 (+)	1.6 (+)	1.1 (+)	1.5 (+)

*Protein sedimented (mg/mL) at 21,000 *g* for 5 min at the end of each incubation period presented in Fig. 3.

†Correlation coefficients between the amounts of aggregated spirals and turbidity for all compounds studied were 0.93 at 0° and 0.93 at 37°.

‡(+) structures were observed, (−) no structures were observed by interference contrast microscopy.

§Correlation coefficients between the amount of aggregated spirals and turbidity for all compounds studied were 0.85 at 37° and 0.81 at 0°.

‖Inactive vinca alkaloid unable to prevent microtubule assembly.

¶Microtubules were observed by electron microscopy.

VCR, VDS, and NVB), and two phosphonates (Fig. 4). These latter were **63**, since it was our model compound, yielding the most uniform aggregated spirals, and **62**, since it had similarities in its behavior to both NVB and VLB. This study was performed at 0°, since the previous findings had demonstrated enhanced aggregated spiral formation with most of these agents at 0° (VLB, VCR, NVB, **62**; see Tables 2 and 3).

With VCR, VDS, and **63** in the absence of MAPs there was little if any evidence for spiral filaments not in large aggregates, since little additional protein was pelleted in the second high-speed centrifugation. As little as 0.6 mg/mL of MAPs resulted in a significant shift of protein from the low-speed to the high-speed pellet (aggregated spirals and spiral filament, respectively). At the highest concentrations of MAPs examined (1.2 and 1.5 mg/mL), this transition was nearly complete: little aggregated spiral material remained, and most of the sedimentable protein had been converted to filaments.

With VLB and pure tubulin, there was only a modestly larger amount of aggregated spirals relative to spiral filaments. At the lowest concentration of MAPs examined (0.3 mg/mL) the aggregated spiral component increased and the spiral filaments decreased. As the MAPs were increased further, however, the aggregated spirals progressively decreased as the filaments increased. At the highest concentrations of MAPs examined, the results with VLB were indistinguishable from those with VCR, VDS, and **63**.

With NVB and **62** with pure tubulin, there was no low-speed pellet, only spiral filaments that were recovered by high-speed centrifugation. With MAPs at 0.3 mg/mL, a significant low-speed pellet was obtained with both compounds, at the expense of the spiral filament component. The amount of protein recovered at 21,000 *g* was somewhat greater with **62** than with NVB, perhaps indicating that turbidity development might be a sigmoidal function of the amount of aggregated spirals formed or of the relative amounts of aggregate and filaments. Similarly to VLB, when the concentration of MAPs was increased further, the aggregated spirals progressively decreased as the filaments increased, and at the highest concentrations examined, the results with NVB and **62** were identical to those with the other compounds.

We next subfractionated the total MAPs to determine whether different components of the preparation had differential activity in the formation of aggregated spirals.

MAP-1 Inhibition of Aggregated Spiral Formation with Compound 63

Studies with fractions enriched for MAP-1A or MAP-1B demonstrated that the two MAP-1 components had nearly equivalent activity in suppressing formation of aggregated spirals induced by our model compound **63** at 0° (Fig. 5). Concentrations as low as 0.15 to 0.2 mg/mL inhibited the reaction by 50%, and nearly complete inhibition occurred by 0.3 mg/mL. The progressive decline in aggregated spirals (21,000 *g* pellet) was accompanied by an equivalent increase in spiral filaments (178,000 *g* pellet).

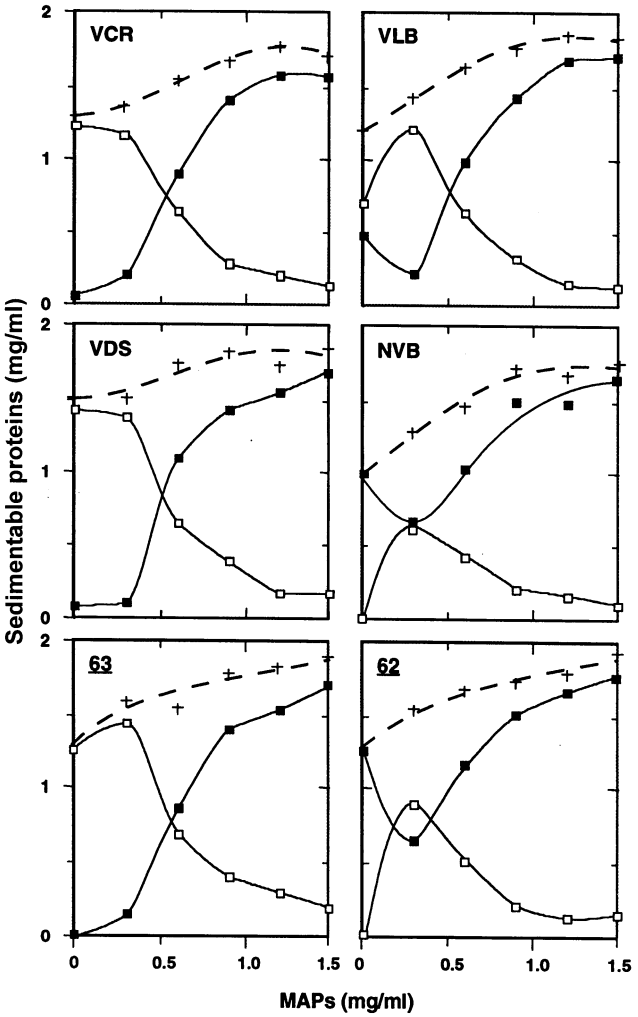

FIG. 4. Variations in the quantities of spiral filaments and aggregated spirals formed in the presence of increasing amounts of total MAPs with different vinca alkaloids. Pure tubulin (1.8 mg/mL) was incubated at 0° in the presence of MAPs (phosphocellulose fraction), and the indicated compound at 100 μM. After 1 hr, 0.1 mL of each incubation mixture was centrifuged (21,000 *g* for 5 min) in order to determine the amount of aggregated spirals in the pellet (open squares). The supernatants were recentrifuged (178,000 *g* for 30 min) in order to determine the amount of spiral filaments (solid squares). The + symbols represent the total protein recovered in the two pellets. The same preparations of tubulin and MAPs were used in all experiments. Typical results of at least three experiments are presented.

MAP-2 and Tau Stimulation of Aggregated Spiral Formation with Compound 62

In contrast to the inhibitory effects of the MAP-1 components on aggregated spiral formation, we found that both MAP-2 and tau stimulated their formation. Compound **62** was selected for detailed study at 0°. This agent was unable to cause aggregated spiral formation with pure tubulin (Table 2, Figs. 2 and 4).

In initial experiments with mixtures of MAPs, we found that unfractionated MAP-1 and a tau–MAP-2 mixture both stimulated aggregated spiral formation with **62**, with

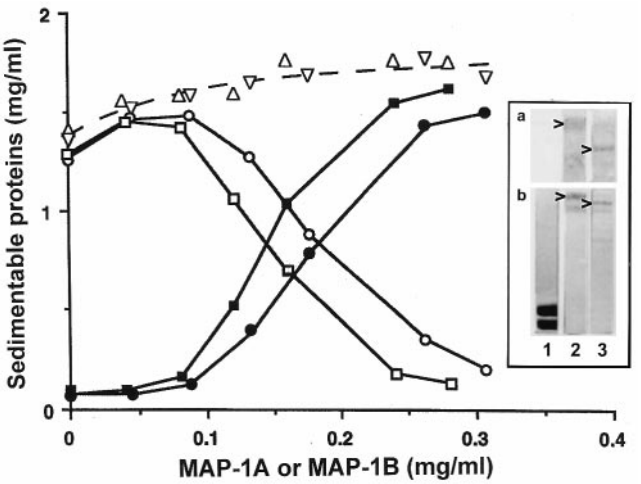

FIG. 5. Variations in the quantity of aggregated spirals formed with compound 63 in the presence of increasing amounts of MAP-1A or MAP-1B. Pure tubulin (1.8 mg/mL) was incubated for 1 hr at 0° in the presence of 100 μM 63 and the indicated amounts of MAP-1A or MAP-1B. The reaction mixtures were successively centrifuged at 21,000 *g* for 5 min and 178,000 *g* for 30 min. Protein contents in the initial and final pellets are indicated by the open and closed squares, respectively, for MAP-1A and the open and closed circles for MAP-1B. The total protein recovered in both pellets is represented by the upright (MAP-1A) and inverted (MAP-1B) triangles. Coomassie blue stained gels are shown in the inset (a, urea/4% acrylamide; b, SDS/6% acrylamide). Lane 1, pure tubulin; lane 2, MAP-1A (arrowheads); lane 3, MAP-1B (arrowheads). The same preparations of MAP-1A, MAP-1B, and tubulin were used in the experiments. Typical results of at least three experiments are presented.

optimal effects at about 0.15 mg/mL. However, with the MAP-1 preparation, pellet size was less than one-fourth of that obtained with the tau–MAP-2 mixture. When we resolved the components of the latter, we found that on a molar basis MAP-2 was 3- to 4-fold more potent than tau (Fig. 6), although there was little difference between the two protein preparations on a weight basis.

DISCUSSION

The effects of high concentrations of thirteen vinca derivatives (all known to strongly inhibit microtubule assembly at low concentrations) allowed the observation of a variety of turbidity patterns as a function of incubation temperature sequence. In nearly all cases, large protein pellets were obtained at 21,000 *g* when there were high turbidity readings, and small pellets were obtained when there were low turbidity readings, regardless of the incubation temperature used. Moreover, when protein was not recovered by centrifugation at 21,000 *g*, it was nevertheless recovered at 178,000 *g*, indicating extensive formation of spiral filaments not incorporated into larger aggregates.

One of the difficulties in studying the effect of vinca alkaloid derivatives is that different workers use different *in vitro* conditions and different protein material. The different conditions used *in vitro* for determination of binding

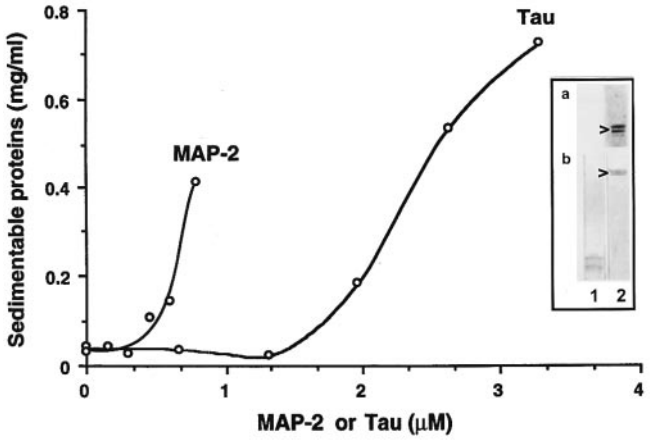

FIG. 6. Variations in the quantity of aggregated spirals formed with compound 62 in the presence of increasing amounts of tau and MAP-2. Pure tubulin (1.8 mg/mL) was incubated for 1 hr at 0° in the presence of 100 μM 62 and the indicated amounts of tau or MAP-2. The reaction mixtures were centrifuged at 21,000 *g* for 5 min, and the amount of protein in the pellets was determined. Coomassie blue stained gels are shown in the inset (a, urea/4% acrylamide; b, SDS/6% acrylamide). Lane 1, tau; lane 2, MAP-2 (arrowheads; the two bands in urea/4% acylamide correspond to the two high molecular weight isoforms of MAP-2). The same preparations of tau, MAP-2, and tubulin have been used in the experiments. Typical results of at least three experiments are presented.

constants of vinca alkaloids are largely responsible for the large range of K_a values found in the literature [3, 27]. The nature and concentration of the buffering component, the ionic strength and the concentration of magnesium of the buffer, as well as the ratio of vinca alkaloid to tubulin are determiners of vinca alkaloids–tubulin interactions, and consequently of the vinca alkaloid-induced tubulin self-association and turbidity development [3, 28].

Magnesium is a major modulator of this process [3, 29]. At the lowest magnesium concentration they used (1 mM), Nogales *et al.* [29] observed that a mixture of spirals and paracrystals is formed at 4°; warming up to 37° induces a growth of spirals and a decrease in the number of paracrystals, consistent with our results. Nevertheless, from 37° to 4°, they observed only a slight increase of aggregation of spirals. But this last temperature shift was subsequent to the 4° to 37° shift, representing a situation potentially different from our individual temperature shifts. Additionally, they used a higher concentration of magnesium (1 vs 0.5 mM) for a similar vinblastine/tubulin ratio (6.1 vs 5.5). At 0.5 mM magnesium, in the presence of microtubule protein, Borman and Kuehne [14] observed isolated spirals and no spiral aggregates, and no turbidity development with 20′-deoxy-20′-desethyl-VLB, which is comparable to what we observed in the presence of 7′-nor-anhydro VLB (NVB). However, they observed an increase of turbidity signal in the presence of VLB at 37°, suggesting the formation of spiral aggregates.

The nature of the nucleotide included in the buffer also influences the degree of polymerization of tubulin by vinca alkaloids [7, 30]. GDP enhances the spiral assembly compared with GTP, by increasing the affinity of liganded tubulin heterodimers for spiral polymers (K_2) and the affinity of vinca alkaloid to unliganded polymers (K_3). Vinca alkaloids inhibit the hydrolysis of GTP by tubulin, so spirals can be formed of tubulin-GTP, but GTP is not required for aggregation [31]. Recently Rai and Wolff [32] described the unspecific electrostatic inhibitory effect of 1 mM GTP, but not 1 mM GDP, on VLB-tubulin spiral cluster formation and on turbidity development at 37°. This is consistent with our observations with VLB and the fact that we included 1 mM GTP in our system. GTP is unstable in aqueous solution, and commercial preparations of GTP present a large range of purities; this could explain why some studies show an increase of turbidity in the presence of VLB at 37° and others, such as this work, do not. Interestingly, Rai and Wolff [32] also observed that when 1 mM GTP is added to preformed VLB-spiral clusters, in the presence of 1 mM magnesium, an abrupt decrease of turbidity occurs, followed by a slow re-increase of turbidity. This is analogous to what we observed, especially in the case of VDS-like compounds, when the temperature was shifted from 0° to 37°. It is tempting to speculate that, when 1 mM GTP is present in the system, the vinca alkaloid spiral clusters might be sensitive to its unraveling effect only at 37°. Moreover, the observations of Rai and Wolff [32] suggest that the presence of spiral cluster seeds left from the 0° incubation would favor the re-association of spirals. Thus, multiple allosteric conformational changes of the tubulin molecule induced by nucleotides, temperature, and different vinca alkaloids influence the ability of spirals to elongate and to cluster through apparently electrostatic interactions [28].

The present study clearly showed that VLB, VCR, VDS, and NVB, despite apparently minimal structural differences, induced significantly different conformational changes of the tubulin protein, which were responsible for differing degrees of spiral aggregation with VCR = VDS > VLB ≫ NVB. Lobert *et al.* [7] were the first to compare quantitatively the interaction of NVB to VCR and VLB with tubulin. They found that all three drugs bind to tubulin heterodimer with the same affinity (K_1) but that affinity of the liganded heterodimer for spirals (K_2) decreases from VCR to NVB, so that the overall affinity (K_1K_2) is the lowest for NVB. Consistent with our data, they observed by analytical ultracentrifugation and stopped flow light scattering at 36° (1 mM magnesium, 0.05 mM GTP) that VCR forms the largest polymers and NVB the smallest, and electron microscopy revealed aggregates of spirals only with VCR. Singer and Himes [15] observed similar differences with VLB, VDS, and VCR by size exclusion HPLC, VDS inducing the formation of polymers intermediate in size between those induced by VCR and VLB. We did not observe significant differences among VCR, VDS, VLB, and NVB in the amount of protein in pellets corresponding to total spirals (free and aggregated spirals). This indicates that each vinca alkaloid induced roughly the same polymer weight, but with different tubulin conformations, i.e. differential exposure of a presumably

charged tubulin domain responsible for spiral clustering. The model for vinca alkaloids binding to tubulin might be even more complex than the ones described, where the drug would have a greater affinity for tubulin in clusters of spirals than in isolated spirals [33, 34]. In accord with the reversible turbidity changes as a function of reaction temperature that we observed with VLB, the time-resolved X-ray solution scattering methodology used by Hodgkinson *et al.* [35] and Nogales *et al.* [29] showed that VLB causes a reversible change in X-ray scattering phenomena. They were able to correlate this change with a reversible 1-nm shift in pitch within the spiral filaments, kinetically following temperature shifts between 4° and 37°. This result indicates that a change of tubulin conformation occurs. Nevertheless, these elegant works do not provide a simple explanation and model fitting our observations.

The correlation between turbidity and low-speed centrifugal protein recovery no longer held up when the thirteen derivatives were evaluated for their effects on microtubule protein as a function of reaction temperature. Low turbidity readings were no longer predictive of negligible protein recovery by centrifugation at 21,000 *g*, although pellets tended to be somewhat smaller when the turbidity readings were low. An explanation of this lack of correlation in the presence of microtubule protein is that MAPs appeared to associate with aggregated spirals and spirals (data not shown), increasing the amount of pelletable proteins without affecting turbidity. Moreover, we (unpublished observations) and other groups [29, 35, 36] observed that in the presence of microtubule protein VLB spirals were formed of two protofilaments, compared with only one in the presence of pure tubulin. Thus, the same amount of spiral aggregates with the same size distribution would scatter light the same way but would represent as much as twice the amount of protein in a low-speed pellet.

MAPs have various actions on vinca alkaloid tubulin spiral as well as paracrystal formation [12, 37]. We found that a high concentration of MAPs caused a substantial reduction in the amount of spiral aggregates but not of spirals. Consequently, little turbidity development was observed (data not shown). This was a specific property of MAP-1 (both MAP-1A and MAP-1B were equivalent inhibitors), while MAP-2 and tau favored formation of larger aggregates. In further studies with **63,** we found that the inhibitory effects of high concentrations of MAPs on aggregated spiral formation occurred only when the MAPs were added to the tubulin before or concomitantly with the alkaloid (not shown). In a recent study, Rai and Wolff [38] described an increase of tubulin aggregation by VLB when the C-terminus of β-tubulin is removed by subtilisin, and no additional effect when the C-terminus of α-tubulin is also removed. This suggests that the acidic C-terminus of β-tubulin interferes with the electrostatic nature of the VLB-induced tubulin aggregation and that MAPs could, similarly to the subtilisin removal, lever the inhibitory effect of the C-terminus. β- and α-tubulin appear to be distinguishable [39]; for example, MAP-2 and tau would interact preferably with the β, and favor aggregation of tubulin dimers by vinca alkaloids, whereas MAP-1 would interact preferably with the α-tubulin C-terminus, inhibiting the formation of spiral aggregates. In this regard, the microtubule binding sequence of MAP-1 is very different from those of MAP-2 and tau, and MAP-1 can be released specifically from the surface of paclitaxel-stabilized microtubules by low concentrations of poly-l-aspartic acid [22].

For the most part, the turbidity patterns obtained with microtubule protein were similar to those obtained with pure tubulin. In particular, this was true with VLB, VDS, NVB, and VCR. Interestingly, each of these four vinca alkaloids used in the treatment of human cancer yielded a distinct turbidity pattern as a function of incubation temperature. With VLB, high turbidity readings were observed at 0°, but not at 37°, and the reaction appeared to be fully reversible. With VDS, high turbidity readings occurred at both temperatures. With NVB, there was no turbidity development at either temperature. VCR presented a mixture of turbidity patterns, VDS-like from 0° to 37° and VLB-like from 37° to 0°.

No obvious structure–activity relationship emerges from our data, but at least some features appear when data in the presence of pure tubulin and microtubule protein are compared by grouping compounds inducing the same type of turbidity patterns in both conditions. NVB is the only compound of its kind in the panel we studied. SAV is the closest compound, but it lacks the important shrinkage of the C′ ring of the velbanamine moiety. Nevertheless, this type of modification as in 20′-deoxy-20′-desethyl VLB [14] seems to generate compounds inducing isolated spirals. Recently Rai and Wolff [40] described VLB-20′-anthranilate as an active compound that interacts with tubulin without even inducing the formation of spirals. Thus, we speculate that some of these modifications at or adjacent to the 20′ carbon on the velbanamine moiety have the greatest influence on the spiral clustering process. VCR was also an isolated case, with a formyl group on the N_a of the vindoline moiety; interestingly, the 20′-deoxyepi VCR or vinepidine has a higher affinity for tubulin than VCR and induces the formation of higher molecular weight polymers [15]. VLB and its analog SAV were in the same group. VDS and its C_{23} *l*-α-amino phosphonate derivatives and the two racemics (Table 1) were in the same group, except for compound S-12129. This compound and the remaining three C_{23} *d*-α-amino phosphonate derivatives of VDS (epimers) did not belong to any of the previous classes headed by one of the four chemotherapeutic vinca alkaloids. S-12363 is the most potent inducer of spiral aggregation, suggesting a greater affinity for tubulin than VCR and indicating that the α-amino phosphonate side-chain has to be aliphatic and in a proper orientation. This characteristic would identify S-12363 as a useful tool in future modeling studies of vinca alkaloid–β tubulin interaction using the recently published structure of the α/β tubulin heterodimer [41]. Finally, we speculate that the differential formation and stability of tubulin spiral aggregates reveal different structural

constraints, which also could act at microtubule ends and result in differential effects on microtubule dynamics [4, 5].

We greatly appreciate the financial support from "L'Association pour la Recherche sur le Cancer" (M. W.) and "La Ligue Nationale contre le Cancer" (P.V-P.). The helpful discussions with Dr. D. Guénard (ICSN, Gif sur Yvette, France) and Dr. E. Hamel (NCI), and the interest of P. Fabre and Servier Laboratories have been highly stimulating.

References

1. Owellen RJ, Donigian DW, Hartke CA and Hains FO, Correlation of biologic data with physico-chemical properties among the vinca alkaloids and their congeners. *Biochem Pharmacol* **26**: 1213–1219, 1977.
2. Himes RH, Interactions of the *Catharanthus* (vinca) alkaloids with tubulin and microtubules. *Pharmacol Ther* **51**: 257–267, 1991.
3. Timasheff SN, Andreu JM and Na GC, Physical and spectroscopic methods for the evaluation of the interactions of antimitotic agents with tubulin. *Pharmacol Ther* **52**: 191–210, 1991.
4. Jordan MA, Thrower D and Wilson L, Effects of vinblastine, podophyllotoxin and nocodazole on mitotic spindles: Implications for the role of microtubule dynamics in mitosis. *J Cell Sci* **102**: 401–416, 1992.
5. Toso RJ, Jordan MA, Farrell KW, Matsumoto B and Wilson L, Kinetic stabilization of microtubule dynamic instability *in vitro* by vinblastine. *Biochemistry* **32**: 1285–1293, 1993.
6. Rowinsky EK and Donehower RC, The clinical pharmacology and use of antimicrotubule agents in cancer chemotherapeutics. *Pharmacol Ther* **52**: 35–84, 1991.
7. Lobert S, Vulevic B and Correia JJ, Interaction of vinca alkaloids with tubulin: A comparison of vinblastine, vincristine, and vinorelbine. *Biochemistry* **35**: 6806–6814, 1996.
8. Hamel E, Interaction of tubulin with small ligands. In: *Microtubule Proteins* (Ed. Avila J), pp. 89–191. CRC Press, Boca Raton FL, 1990.
9. Mackinlay SA, Ludueña RF and MacRae TH, Vinblastine-induced aggregation of brine shrimp (*Artemia*) tubulin. *Biochim Biophys Acta* **882**: 419–426, 1986.
10. Takanari H, Yosida T, Morita J, Isutzu K and Ito T, Instability of pleomorphic tubulin paracrystals artificially induced by vinca alkaloids in tissue-cultured cells. *Biol Cell* **70**: 83–90, 1990.
11. Himes RH, Kersey RN, Heller-Bettinger I and Samson FE, Action of the *Vinca* alkaloids vincristine, vinblastine and desacetyl vinblastine amide (vindesine) on microtubules *in vitro*. *Cancer Res* **36**: 3798–3802, 1976.
12. Ludueña RF, Fellous A, Francon J, Nunez J and McManus L, Effect of tau on the vinblastine-induced aggregation of tubulin. *J Cell Biol* **89**: 680–683, 1981.
13. Ludueña RF, Fellous A, McManus L, Jordan MA and Nunez J, Contrasting roles of tau and microtubule-associated protein 2 in the vinblastine-induced aggregation of brain tubulin. *J Biol Chem* **259**: 12890–12898, 1984.
14. Borman L and Kuehne ME, Specific alterations in the biological activities of C-20′-modified vinblastine congeners. *Biochem Pharmacol* **38**: 715–724, 1989.
15. Singer WD and Himes RH, Cellular uptake and tubulin binding properties of four vinca alkaloids. *Biochem Pharmacol* **43**: 545–551, 1992.
16. Müller LJ, Moorer-van Delft CM, Zijl R and Roubos EW, Use of snail neurons in developing quantitative ultrastructural parameters for neurotoxic side effects of *Vinca* antitumor agents. *Cancer Res* **50**: 1924–1928, 1990.
17. Delbarre B, Granger C, Grosse R, Wright M, Paraire M and Bizzari JP, S-12363 a new vinca-alkaloid derivative inducing spiralization of microtubules. *Proceedings of the 81st Annual Meeting of the American Association for Cancer Research*, Washington DC, U.S.A., 23–26 May 1990, Vol. 31, p. 401b. American Association for Cancer Research, Philadelphia, PA, 1990.
18. Wright M, Garès M, Verdier-Pinard P, Moisand A, Berlion M, Legrand JJ and Bizzari JP, Differential *in vitro* action of S-12363, a new vinblastine derivative, and of its epimer on microtubule proteins. *Cancer Chemother Pharmacol* **28**: 434–440, 1991.
19. Lavielle G, Hautefaye P, Schaeffer C, Boutin JA, Cudennec CA and Pierré A, New α-amino phosphonic acid derivatives of vinblastine: Chemistry and antitumor activity. *J Med Chem* **34**: 1998–2003, 1991.
20. Shelanski ML, Gaskin F and Cantor CL, Microtubule assembly in the absence of added nucleotides. *Proc Natl Acad Sci USA* **70**: 765–768, 1973.
21. Weingarten MD, Lockwood AH, Hwo SY and Kirschner MW, A protein factor essential for microtubule assembly. *Proc Natl Acad Sci USA* **72**: 1858–1862, 1975.
22. Fujii T, Nakamura A, Ogoma Y, Kondo Y and Arai T, Selective purification of microtubule-associated proteins 1 and 2 from rat brain using poly(l-aspartic acid). *Anal Biochem* **184**: 268–273, 1990.
23. Bloom GS, Lucas FC and Vallee RB, Identification of a major component of the neuronal cytoskeleton. *Proc Natl Acad Sci USA* **82**: 5404–5408, 1985.
24. Zavala F, Guénard D and Potier P, Interaction of vinblastine analogues with tubulin. *Experientia* **34**: 1497–1499, 1978.
25. Nimni ME, Vinblastine sulfate: Its reversible thermal aggregation and interaction with hydrophobic groups. *Biochem Pharmacol* **21**: 485–493, 1972.
26. Ventilla M, Cantor CR and Shelanski ML, Some features of the vinblastine-induced assembly of porcine tubulin. *Arch Biochem Biophys* **171**: 154–162, 1975.
27. Singer WD, Hersh RT and Himes RH, Effect of solution variables on the binding of vinblastine to tubulin. *Biochem Pharmacol* **37**: 2691–2696, 1988.
28. Lobert S, Boyd CA and Correia JJ, Divalent cation and ionic strength on *Vinca* alkaloid-induced tubulin self-association. *Biophys J* **72**: 416–427, 1997.
29. Nogales E, Medrano FJ, Diakun GP, Mant GR, Towns-Andrews E and Bordas J, The effect of temperature on the structure of vinblastine-induced polymers of purified tubulin: Detection of a reversible conformational change. *J Mol Biol* **254**: 416–430, 1995.
30. Lobert S, Frankfurter A, and Correia JJ, Binding of vinblastine to phosphocellulose-purified and αβ-class III tubulin: The role of nucleotides and β-tubulin isotypes. *Biochemistry* **34**: 8050–8060, 1995.
31. David-Pfeuty T, Simon C and Pantaloni D, Effect of antimitotic drugs on tubulin GTPase activity and self-assembly. *J Biol Chem* **254**: 11696–11702, 1979.
32. Rai SS and Wolff J, Vinblastine-induced formation of tubulin polymers is electrostatically regulated and nucleated. *Eur J Biochem* **250**: 427–431, 1997.
33. Bryan J, Definition of three classes of binding sites in isolated microtubule crystals. *Biochemistry* **11**: 2611–2616, 1972.
34. Wilson L, Morse ANC and Bryan J, Characterization of *acetyl*-^{3}H-labeled vinblastine binding to vinblastine-tubulin crystals. *J Mol Biol* **121**: 255–268, 1978.
35. Hodgkinson JL, Hutton T, Medrano FJ and Bordas J, X-ray solution scattering studies on vinblastine-induced polymers of microtubule protein: Structural characterisation and effects of temperature. *J Struct Biol* **109**: 28–38, 1992.
36. Amos LA, Jubb JS, Henderson R and Vigers G, Arrangement

of protofilaments in two forms of tubulin crystal induced by vinblastine. *J Mol Biol* **178**: 711–729, 1984.
37. Donoso JA, Haskins KM and Himes RH, Effect of microtubule-associated proteins on the interaction of vincristine with microtubule and tubulin. *Cancer Res* **39:** 1604–1610, 1979.
38. Rai SS and Wolff J, The C terminus of β-tubulin regulates vinblastine-induced tubulin polymerization. *Proc Natl Acad Sci USA* **95**: 4253–4257, 1998.
39. Sackett DL, Structure and function in the tubulin dimer and the role of the acidic carbonyl terminus. In: *Subcellular Biochemistry* (Eds. Biswas BB and Siddhartha R), Vol. 24, pp. 255–302. Plenum Press, New York, 1995.
40. Rai SS and Wolff J, Dissociation of tubulin assembly-inhibiting and aggregation-promoting activities by a vinblastine derivative. *FEBS Lett* **416**: 251–253, 1997.
41. Nogales E, Wolf SG and Downing KH, Structure of the αβ tubulin dimer by electron crystallography. *Nature* **391**: 199–202, 1998.